Research Article

Huijun Duan, Shijun Hao*, Jie Feng*, Yi Wang, and Dong Peng

A prediction method for water enrichment in aquifer based on GIS and coupled AHP–entropy model

https://doi.org/10.1515/geo-2020-0277
received January 20, 2021; accepted July 08, 2021

Abstract: To prevent coal mine water disasters, the main objective of this study is to predict the water enrichment of the main aquifer in a coal mine of China that has been threatened by water inrush. The prediction is carried out using a geographic information system (GIS) and a coupled analytic hierarchy process (AHP) and entropy model. The flushing fluid consumption, burnt rock distribution, sand–shale ratio, and lithology structure index were determined as the main factors controlling the water enrichment of the aquifer. A thematic map of these main factors was constructed using the spatial data analysis functions of GIS and the data from a total of 146 drilling columns and field investigation. The weights of these controlling factors were calculated using the coupled model. A prediction map of the water enrichment of the aquifer was then developed by overlaying the thematic map with the weights of each controlling factor. The degree of water enrichment was finally divided into four levels for easy interpretation, where Level I denotes the highest water enrichment and poses the greatest threat of water disaster.

Keywords: water enrichment, aquifer, AHP, entropy method, coal mine

*** Corresponding author: Shijun Hao,** China Coal Research Institute, Beijing 100013, China; Xi'an Research Institute, China Coal Technology and Engineering Group, Research and development center, Xi'an 710077, China, e-mail: shijunhaoccr@outlook.com
*** Corresponding author: Jie Feng,** Department of Hydrogeology, China Coal Energy Research Institute Co Ltd, Xi'an, Shaanxi 710054, China, e-mail: jiedong07198@163.com
Huijun Duan: China Coal Research Institute, Beijing 100013, China; Department of Drilling Technology and Engineering, Xi'an Research Institute, China Coal Technology and Engineering Group, Xi'an 710077, China
Yi Wang, Dong Peng: Department of Drilling Technology and Engineering, Xi'an Research Institute, China Coal Technology and Engineering Group, Xi'an 710077, China

1 Introduction

Water inrush to a coal mine is a water disaster that can significantly impact the safe operations of coal mines in China [1]. According to statistics collected between 2011 and 2016 in China, there was a total of 72 water inrushes to coal mines, which caused 18.4% more accidents and 17.6% large-scale accidents compared to workplace accidents across the whole China. These inrushes also caused 449 deaths. As the intensity of mining continues to increase with the strategy to develop western China, water inrushes from aquifer roofs to coal mines have serious consequences [2]. The water flowing in the fractured zone and the water enrichment of the aquifer are two important factors in water inrush in coal mines, and the degree of water enrichment directly determines the amount and duration of water inrush. Hence, the selection of the area of the aquifer with abnormal water enrichment is critical. Many scholars have conducted studies on water inrush prevention and mainly considered the following two indicators in the selection of the area of the aquifer: the first is specific capacity, which is obtained by a pumping test and is the most accurate and direct parameter that can be used to evaluate the water enrichment of the aquifer; the second is the multi-information superposition based on the geographic information system (GIS) and mathematical models. Over the past two decades, the GIS has been widely used in various fields [3–7]. The GIS has also been used by hydrologists to predict water inrushes to coal mines [8–10]. Moreover, with the rapid development of computers, many researchers are employing mathematical approaches [8,11–26], such as the analytic hierarchy process (AHP), fuzzy theory, and artificial neural networks, to predict the water enrichment of aquifers and water hazards. The "three maps–two predictions" quantitative assessment method has been commonly used to predict groundwater intrusion from overlying aquifers. One of the maps in the "three maps–two predictions" method is the prediction map of the water enrichment of the aquifer.

In the preceding literature review, it can be seen that there are problems facing the prediction of water enrichment: (1) while the specific capacity is the most direct and accurate parameter to judge water enrichment, it has poor reliability, is time consuming, and comes with high costs due to the drilling process; (2) the factors controlling water enrichment vary across mining areas, and thus, we should choose the main factors found to control water enrichment across geological and mining conditions; (3) there are few studies on water inrush from an overlying aquifer to a coal seam. Therefore, the objective of this study is to use the GIS and a coupled AHP–entropy model to predict the water enrichment of the aquifer overlying the first layer of the coal seam in a coal mine in China. This study is very useful because water inrush accidents only occur when mining is carried out underneath a water-rich area.

2 Study area

The coal mine utilized in the present study covers an area of 51.9798 km^2; it is located in Shenmu County, Shaanxi Province, China, within latitudes 38°57′38″N–39°1′37″N and longitudes 110°16′21″E–110°23′31″E (Figure 1). The altitude of the coal mine varies from 1088.0 to 1302.9 m, and it is located in a transition zone from aeolian landforms to hilly loess regions. Wulanbula Spring and Laolai Creek converge to form the only perennial river in this area. According to data from the Shenmu County meteorological station, the average annual evaporation is 1774.1 mm, and the rainfall is 436.6–553.1 mm. The main rainy months are from July to September.

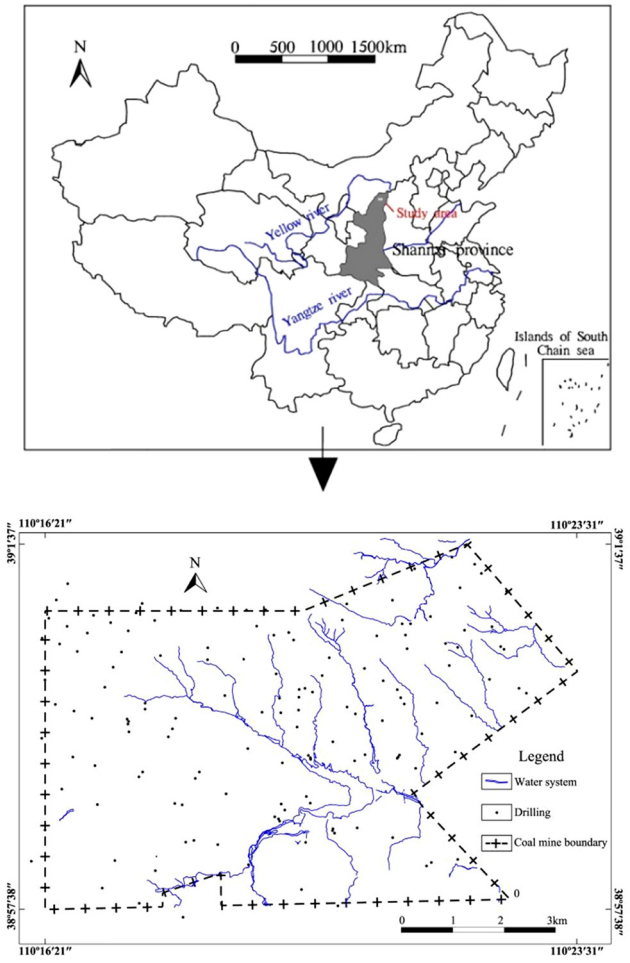

Figure 1: Location and water system of the coal mine.

2.1 Geological conditions

Based on the exploration data, the stratigraphy of the area from bottom to top is the Triassic system, Jurassic system, Neogene system, and Quaternary system (Figures 2 and 3). Furthermore, the Yanan Formation of the Middle Jurassic is the main coal-bearing strata. These strata contain seven recoverable coal seams; the minable coal seams are Nos. 3^{-1}, 4^{-2}, and 5^{-2}, with an average thickness of 4.11 m and buried depth ranging from 0 to 302.72 m. The stratigraphic dip of the strata in the coal mine is 1–2° with a monoclinal structure inclined toward the northwest.

2.2 Hydrogeological conditions

In the mining area, there are two types of aquifers. The first is the Quaternary unconsolidated layer and porous aquifer, which includes the alluvium–diluvium of the Holocene Series, the Salawusu Formation of Upper Pleistocene, and the loess layer of Middle–Upper Pleistocene. The second aquifer is the bedrock fissure aquifer of the Jurassic period; this aquifer includes the Zhiluo Formation of the Middle Jurassic, and the Yan'an Formation of the Middle Jurassic. Figure 2 shows a breakdown of typical geologic systems.

The main aquifer of the coal mine is in the Salawusu Formation. Based on the drilling record, it is 10–23 m thick. From the hydrological drill hole, the water level elevation of this aquifer is about 5 m. The specific capacity is less than 1.47 L·(s·m)$^{-1}$, and the salinity of the water is less than 0.187 g/L. In addition, there is a special type of rock called burnt rock, which is formed in the distribution area near the surface of a combustible coal

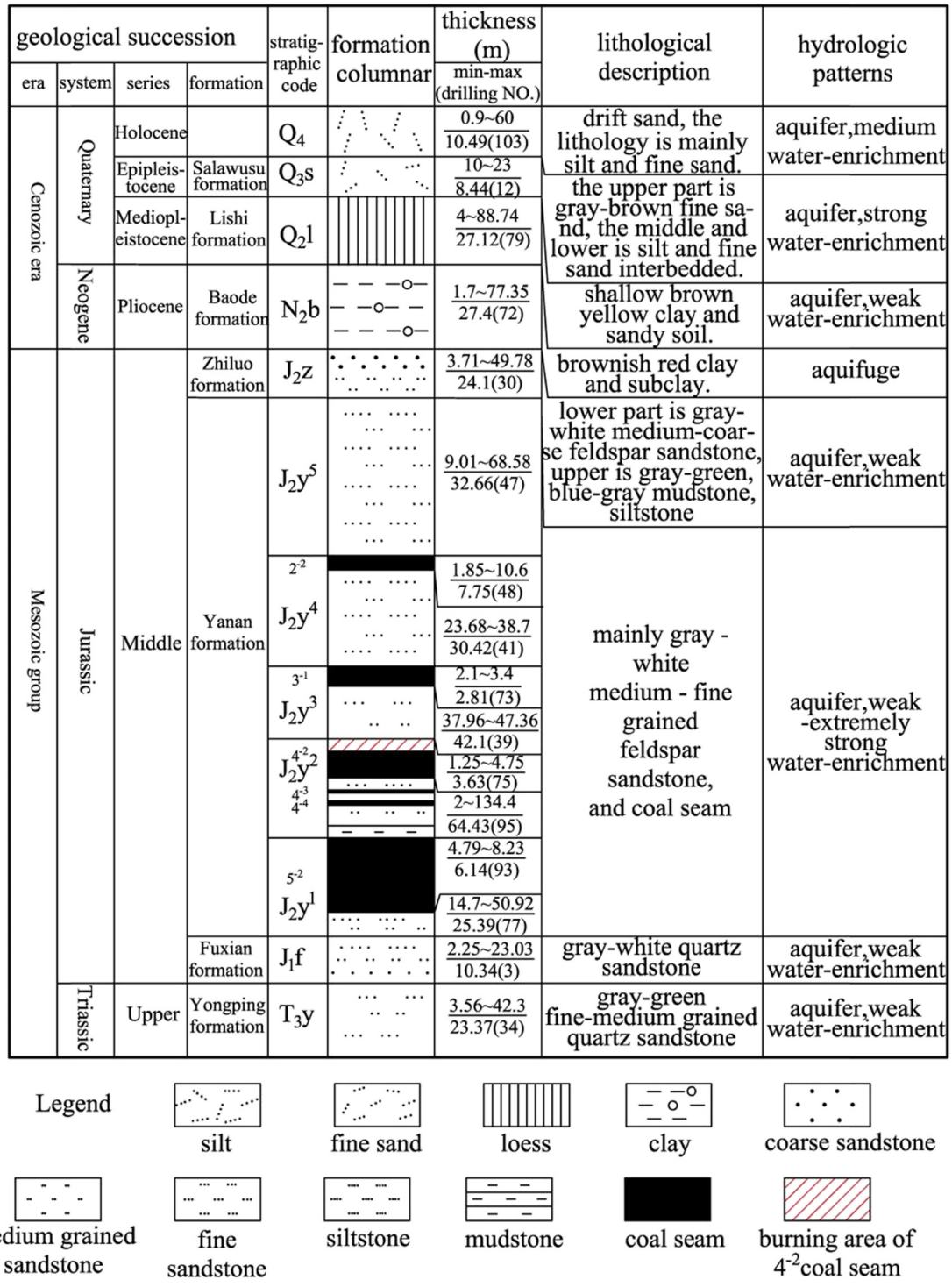

Figure 2: Breakdown of the aquifers and aquifuges in the coal mine.

seam. Coal spontaneous combustion occurs under appropriate external conditions. During spontaneous combustion, the coal seam itself burns, and part or all becomes coal ash; its surrounding rock is also roasted to form burnt rock. This phenomenon is also called self-burning and is common across the world. There is a large number of pores in the burnt rock, and such rock is widely exposed in valley areas (Figure 4(b)). Water flowing through the fractures and reaching the burnt rock during mining can result in disaster. According to simple hydrogeology observations made during drilling, the thickness of the burnt rock is 15–30 m, and the maximum leakage is

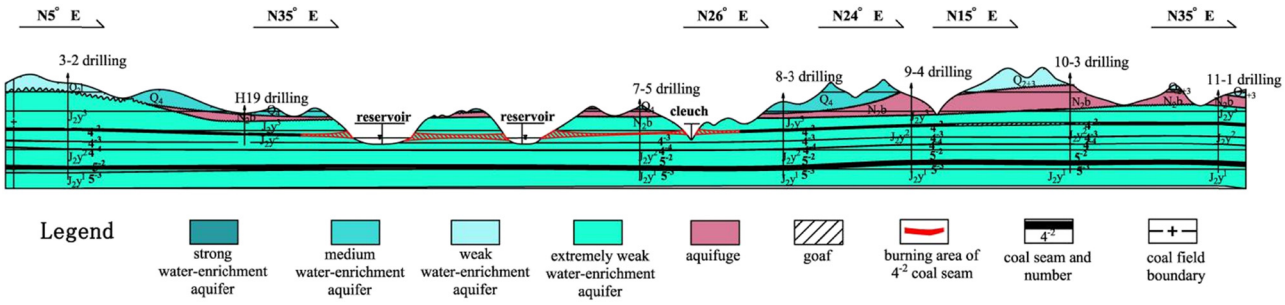

Figure 3: Runoff discharge of the coal mine.

15 m^3/h. Figure 3 shows the hydrogeologic profile of the coal mine.

3 Methodology

3.1 AHP

The AHP is a multi-objective decision method proposed by Thomas Satty at the University of Pennsylvania in the United States. This method is used to analyze major controlling factors, assigns expert scores to these factors, and combines quantitative and qualitative decisions. The key to the AHP is the comparisons between alternatives with regards to subcriteria, between subcriteria with regards to criteria, and between criteria with regards to primary goals; these comparisons are made by attributing weights to judgments. The AHP has been widely used in all walks of life to solve many decision problems. There are many factors affecting the water enrichment of the aquifer, and the weight of each factor can be determined by the AHP [10]. By determining these weights, we can guide the prevention of mine water disasters.

The calculation processes are as follows:

- Develop a hierarchical model
- Construct a judgment matrix
- Calculate the weight vector and carry out a consistency check

The consistency check by single sorting (C.I.) can be carried out using the following formula:

$$\text{C.I.} = \frac{\lambda_{\max} - n}{n - 1}. \tag{1}$$

The consistency check of total sorting (C.R.) can be carried out using the following formula:

$$\text{C.R.} = \frac{\sum_{j=1}^{m} \text{C.I.}_{ja_j}}{\sum_{j=1}^{m} \text{R.I.}_{ja_j}}, \tag{2}$$

where the maximum eigenvalue of the judgment matrix is represented by $\lambda_{\max}$, the number of factors in the index layer is represented by n, the number of factors in the criterion layer is represented by m, the jth factor in the criterion layer is represented by j, the weight of the jth factor between the criterion layer and target layer is represented by a_j, the consistency index of the judgment matrix in the index layer corresponding to a_j is represented by C.I._j, and the random index of the judgment matrix in the index layer corresponding to a_j is represented by R.I._j. When C.R. <0.1, the judgment matrix is reasonable and satisfies the consistency test.

3.2 Entropy method

The concept of entropy was first proposed by the German physicist R. Clausius in 1865. Entropy is a measurement of the disorder of a system, and the entropy method is a type of comprehensive evaluation method for multiple objects and multiple indices. The evaluation results are mainly based on objective data and are almost uninfluenced by subjective factors. Hence, human factors are avoided to a large extent. This method can compensate for the subjective factors of the AHP and objectively reflect the influence weight of each factor on water enrichment. Some scholars have applied it to the organic Rankine cycle system [25].

In this method, we first determine the object to be evaluated and construct a horizontal index matrix $R = (r_{ij})_{m\times n}$. Then, we calculate the weight of each index.

The ratio of the index of the ith object under jth index can be calculated using the following formula:

$$P_{ij} = \frac{r_{ij}}{\sum_{i=1}^{m} r_{ij}}. \tag{3}$$

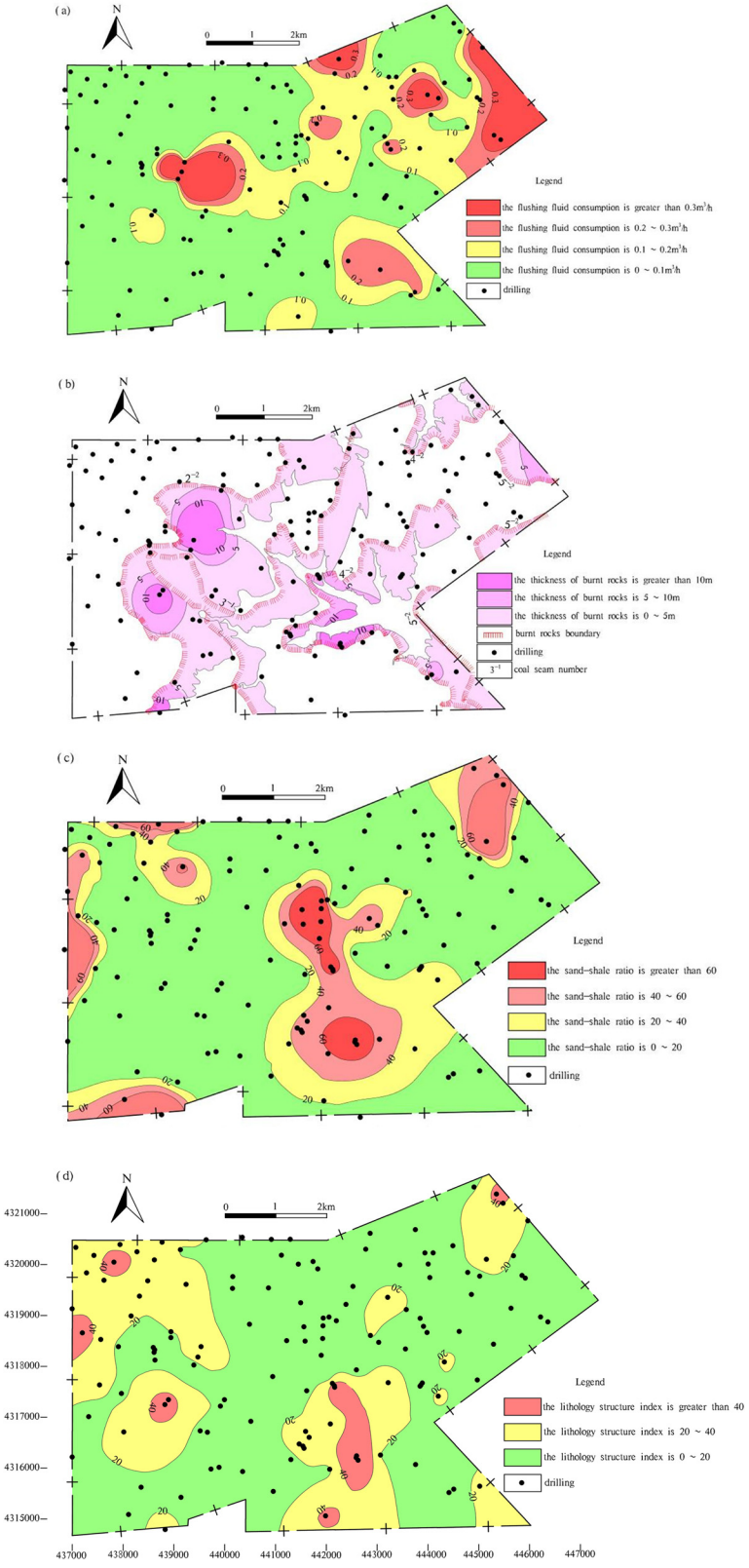

Figure 4: Thematic maps of each major controlling factor: (a) flushing fluid consumption, (b) distribution and thickness of burnt rock, (c) sand–shale ratio, and (d) lithology structure index.

The entropy of the jth index can be calculated using the following formula:

$$e_j = -k\sum_{i=1}^{m} p_{ij} \cdot \ln p_{ij} \begin{cases} p_{ij} = \dfrac{r_{ij}}{\sum_{i=1}^{m} r_{ij}}, & k = \dfrac{1}{\ln m}. \\ p_{ij} \cdot \ln p_{ij} = 0, & p_{ij} = 0 \end{cases} \quad (4)$$

The entropy weight of the jth index can be calculated using the following formula:

$$w_j = \frac{1 - e_j}{\sum_{j=1}^{n}(1 - e_j)}, \quad (5)$$

where r_{ij} is the estimated value of the ith object under the jth index, m is the number of objects evaluated, and n is the number of evaluation indices.

3.3 The coupled model

The coupled model combines the subjective weights obtained by the AHP with the objective weights obtained using the entropy method. The value of the comprehensive evaluation for the investigated factors, β_j, can be calculated as follows:

$$\beta_j = a_j \cdot w_j, \quad (6)$$

where α_j ($j = 1, 2, \cdots, n$) is the weighted value obtained by the AHP.

The weighted value of the comprehensive evaluation, Z_j, of the factors can be calculated as follows:

$$Z_j = \frac{\beta_j}{\sum_{j=1}^{n}\beta_j}. \quad (7)$$

The final calculation results can then be obtained based on the principle of maximum membership.

4 Construction of the coupled model

4.1 Determination of major controlling factors

The reliability of the final prediction results must be considered alongside the fact that geological and hydrogeological conditions are different in different mines and thus the results are dependent on many factors [28]. Reasonable determination of the major controlling factors is the key to ensuring prediction reliability. Through assessment of hydrogeological and mining conditions in the studied mine, we determine that the four major controlling factors are the flushing fluid consumption, distribution and thickness of burnt rock, sand–shale ratio, and the lithology structure.

The flushing fluid consumption is the amount of flushing medium returned during drilling and reflects the degree of rock fragmentation. There is a positive correlation between the flushing fluid consumption and water enrichment, and the greater the flushing fluid consumption, the stronger the water enrichment. Burnt rock is a special stratum in the study area and is widely developed in shallow coal seams. This burnt rock can be divided into burnt lava, sintered rock, and baked rock. The main characteristics of these rocks are porosity and strong water enrichment. Note that the distribution and thickness of burnt rock are important for aquifer water enrichment prediction. Furthermore, it is generally believed that the higher the sandstone content, the stronger the water enrichment of the aquifer; therefore, the sand–shale ratio is another main factor affecting water enrichment. Finally, it is well known that the larger the rock particles, the stronger the water enrichment, and hence, rock lithology is another main controlling factor. This factor is expressed by the lithology structure index.

The lithology structure index can be calculated by the thicknesses of the coarse sandstone, medium sandstone, fine sandstone, and siltstone, and by multiplying by their respective equivalent coefficients. This converts the thicknesses of the medium sandstone, fine sandstone, and siltstone into the thickness of the coarse sandstone, and then multiplies it by the structure coefficient (E). The lithology structure index (L) is defined as follows:

$$L = (a \times 1 + b \times 0.8 + c \times 0.6 + d \times 0.4) \times E, \quad (8)$$

where a, b, c, and d are the thicknesses of the coarse sandstone, medium sandstone, fine sandstone, and siltstone, respectively; and E is determined from the composition structure of the sandstone and mudstone. The value of E corresponds to the ratio of the total sandstone thickness and the rock formation thickness, as presented in Table 1.

We note here that the burnt rock thickness is equivalent to the coarse sandstone thickness.

4.2 Development of thematic maps

The prediction of water enrichment is highly dependent on the aquifer and can guide water detection and water release during mining operations. In this study, the

Table 1: Values of E corresponding to the ratio of total sandstone thickness and rock formation thickness

Total sandstone thickness/rock formation thickness (%)	E
>90	1
70–90	0.8
50–70	0.6
30–50	0.4
<30	0.2

bedrock from the top of the first coal seam to the bottom of the loose layer is considered as a unified aquifer group. This is because the bedrock is mainly composed of sand with some mud. Based on the aforementioned major controlling factors, and the available geological and hydrogeological data from a total of 146 drillings, we construct thematic maps using the software MapGIS 6.7. A thematic map can be developed for each major controlling factor, thereby allowing us to illustrate the distribution and attributes of each factor. Figure 4 presents the thematic maps for the flushing fluid consumption, distribution and thickness of burnt rock, sand–shale ratio, and lithology structure index.

From Figure 4(a), it can be seen that the maximum flushing fluid consumption is located at the central and northeast parts of the coal mine. The flushing fluid consumption is generally between 0.1 and 0.3 m^3/h. This is proportional to the water enrichment. Meanwhile, Figure 4(b) shows the distribution and thickness of the burnt rock, which is also proportional to the water enrichment. For a thicker and larger distribution of the burnt rock, the water enrichment is greater. The thickness of the burnt rock is generally 5–10 m. Figure 4(c) displays the relationship between the sand–shale ratio and water enrichment, while Figure 4(d) shows the relationship between the lithology structure index and water enrichment. Note that the increased presence of gritstone corresponds to greater water enrichment.

5 Results

5.1 Calculation of weighted factors by the coupled model

Following the determination of the major controlling factors, a judgment matrix A is constructed by the expert scoring method. The water enrichment of the aquifer is the target layer, and the flushing fluid consumption, burnt rock, sand–shale ratio, and lithology structure index comprise the criteria layer.

$$A = \begin{bmatrix} 1 & 2 & 5 & 4 \\ 1/2 & 1 & 4 & 5 \\ 1/5 & 1/4 & 1 & 3 \\ 1/4 & 1/5 & 1/3 & 1 \end{bmatrix}$$

In judgment matrix A, in the first row from left to right and the first column from top to bottom are the flushing fluid consumption, burnt rock, sand–shale ratio, and lithology structure indices. The values in the first row and the third column indicate that the sand–shale ratio has a greater contribution to water enrichment than the flushing fluid consumption; the opposite can be observed by the values in the first column and the third row.

The consistency of the matrix is checked using equations (1) and (2), and it satisfies the consistency requirements. Using equations (3)–(5), data from the 146 drillings, and the weights of the factors obtained by the entropy method, the horizontal matrix $R = (r_{ij})_{m\times n}$ is constructed. Finally, the weights of the controlling factors are calculated and are presented in Table 2.

5.2 Prediction of water enrichment of the aquifer overlying the first coal seam

By using the MapGIS 6.7 layer overlay function to overlay each thematic map with the weights of the controlling factors, the water enrichment of the aquifer overlying the first coal seam in the coal mine can be determined. The mathematical model for the prediction is as follows:

$$\begin{aligned} &\text{Water enrichment } (E) \\ &= \text{Flushing fluid consumption} \times 0.475 \\ &\quad + \text{Burnt rock} \times 0.431 + \text{Sand–shale ratio} \\ &\quad \times 0.085 + \text{Lithology structure index} \times 0.009. \end{aligned} \tag{9}$$

The specific capacity is an important index that reflects the degree of water enrichment. However, the specific capacity data is limited. Thus, the prediction result is verified using both the specific capacity and the water inrush events. Moreover, since the specific capacity is the most accurate prediction method, it complements the coupled model well. The degrees of water enrichment can be expressed via the levels listed below.

Level I: On this level, $[E] > 2.5$, and it indicates the highest water enrichment. This is mainly observed in the central and eastern parts of the coal mine. There are four regions of the mine that are Level I,

Table 2: Weights of the controlling factors

Controlling factors	Weights of the controlling factors		
	Obtained by the AHP (α_i)	Obtained by the entropy method (ω_j)	Obtained by the coupled model (Z_j)
Flushing fluid consumption	0.477	0.317	0.475
Burnt rock	0.337	0.408	0.431
Sand–shale ratio	0.118	0.228	0.085
Lithology structure index	0.068	0.047	0.009

constituting a total area of 3.48 km^2 and accounting for 6.7% of the total coal mine area.

Level II: For this level, the [E] ranges between 1.88 and 2.5. Level II is mainly observed in the central and eastern parts of the coal mine. There are seven regions of the mine that are Level II, constituting a total area of 5.98 km^2 and accounting for 11.51% of the total coal mine area.

Level III: For this level, the [E] is between 1.25 and 1.88. Level III areas are mainly found surrounding Level II areas. There are six Level III regions, constituting a total area of 14.05 km^2 and accounting for 27.03% of the total coal mine area.

Level IV: This level corresponds to a [E] ≤ 1.25 and denotes the lowest water enrichment. Level IV areas are found in the western, southern, and eastern parts of the coal mine. There are two Level IV regions, constituting a total area of 28.46 km^2 and accounting for 54.76% of the total coal mine area.

Using the coupled model, the prediction of the water enrichment is divided into the aforementioned four levels. The water enrichment thresholds are at 1.25, 1.88, and 2.5. The lower the level, the greater the water enrichment. This is an indication that it is easier for a water inrush event to happen. Figure 5 shows the prediction map of the water enrichment of the aquifer overlying the first coal seam.

6 Discussion

The prediction of the water enrichment of the aquifer overlying the first coal seam in the studied coal mine is

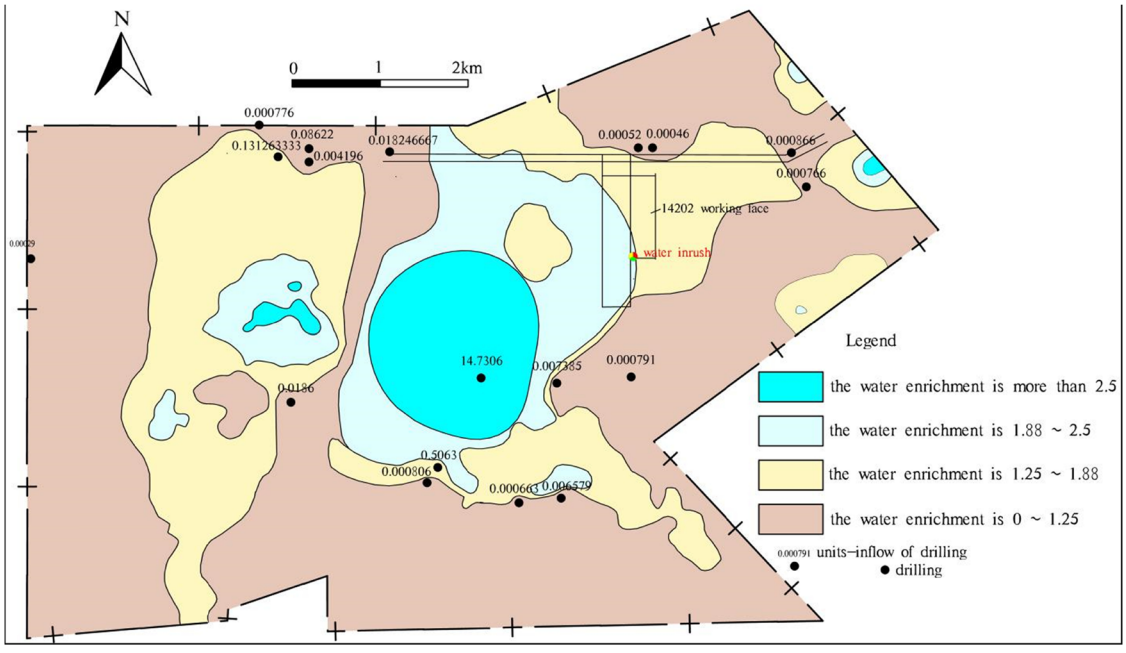

Figure 5: Prediction map of the water enrichment of the aquifer overlying the first coal seam in the studied coal mine.

Table 3: Prediction results compared with historical data of water inrush events and recorded specific capacity

No.	Place	Specific capacity $L\cdot(s\cdot m)^{-1}$	Water inrush event	Prediction result	Regulations for prediction of water enrichment of the aquifer by specific capacity
1	14,202 working face	—	Water inrush	Level II	—
2	In the northwest	0.000766–0.08622	—	Level IV	$\leq 0.1\ L\cdot(s\cdot m)^{-1}$, Level IV
3	In the northwest	0.131263	—	Level III	$0.1–1\ L\cdot(s\cdot m)^{-1}$, Level III
4	In the northeast	0.00046–0.00086	—	Level IV	$\leq 0.1\ L\cdot(s\cdot m)^{-1}$, Level IV
5	In the middle	0.000791–0.0186	—	Level IV	$\leq 0.1\ L\cdot(s\cdot m)^{-1}$, Level IV
6	In the middle	14.7306	—	Level I	$>5\ L\cdot(s\cdot m)^{-1}$, Level I
7	In the south	0.0006579–0.000806	—	Level IV	$\leq 0.1\ L\cdot(s\cdot m)^{-1}$, Level IV
8	In the south	0.5063	—	Level III	$0.1–1\ L\cdot(s\cdot m)^{-1}$, Level III

Table 4: Assessment of reliability of prediction results

Prediction result	Specific capacity $L\cdot(s\cdot m)^{-1}$	Reliability of prediction result
Level IV	0.000776	Specific capacity $\leq 0.1\ L\cdot(s\cdot m)^{-1}$, reliable
Level IV	0.08622	Specific capacity $\leq 0.1\ L\cdot(s\cdot m)^{-1}$, reliable
Level IV	0.004196	Specific capacity $\leq 0.1\ L\cdot(s\cdot m)^{-1}$, reliable
Level III	0.131263	Specific capacity $0.1–1\ L\cdot(s\cdot m)^{-1}$, reliable
Level IV	0.018247	Specific capacity $\leq 0.1\ L\cdot(s\cdot m)^{-1}$, reliable
Level IV	0.00052	Specific capacity $\leq 0.1\ L\cdot(s\cdot m)^{-1}$, reliable
Level IV	0.00046	Specific capacity $\leq 0.1\ L\cdot(s\cdot m)^{-1}$, reliable
Level IV	0.000866	Specific capacity $\leq 0.1\ L\cdot(s\cdot m)^{-1}$, reliable
Level IV	0.000766	Specific capacity $\leq 0.1\ L\cdot(s\cdot m)^{-1}$, reliable
Level I	14.7306	Specific capacity $>5\ L\cdot(s\cdot m)^{-1}$, reliable
Level IV	0.007385	Specific capacity $\leq 0.1\ L\cdot(s\cdot m)^{-1}$, reliable
Level IV	0.000791	Specific capacity $\leq 0.1\ L\cdot(s\cdot m)^{-1}$, reliable
Level IV	0.006579	Specific capacity $\leq 0.1\ L\cdot(s\cdot m)^{-1}$, reliable
Level IV	0.000663	Specific capacity $\leq 0.1\ L\cdot(s\cdot m)^{-1}$, reliable
Level III	0.5063	Specific capacity $0.1–1\ L\cdot(s\cdot m)^{-1}$, reliable
Level IV	0.000806	Specific capacity $\leq 0.1\ L\cdot(s\cdot m)^{-1}$, reliable
Level IV	0.0186	Specific capacity $\leq 0.1\ L\cdot(s\cdot m)^{-1}$, reliable

shown in Figure 5. To further verify the prediction's accuracy, the prediction results are compared with the measured historical data of water inrush events and specific capacity (Table 3). We also specifically assess the reliability of the prediction results using the specific capacity (Table 4). As Table 4 shows, the accuracy of the prediction results is 100%, indicating that the coupled model can be used to predict the water enrichment in coal mines under conditions similar to those in the present case.

7 Conclusion

The coupled AHP–entropy model was evaluated with respect to its ability to reliably predict the water enrichment of the aquifer overlying the first coal seam of a specific coal mine in China. The flushing fluid consumption, burnt rock distribution, sand–shale ratio, and lithology structure index were selected as the main factors controlling water enrichment. Based on 146 drilling columns and field investigation in the study area, four thematic maps of the major controlling factors were completed using the software MapGIS 6.7. According to the AHP and the entropy method, the weights of these controlling factors were calculated. A mathematical model for the prediction of the water enrichment was then generated. Finally, the prediction map of the water enrichment of the aquifer overlying the first coal seam in the coal mine was completed using MapGIS 6.7. The prediction map was divided into four levels according to the degree of water enrichment; Level I denoted the highest water enrichment, and Level IV denoted the lowest. These prediction results were compared to the recorded water inrush event in the 14,202 working face and the specific

capacity at this working face; this showed the approach to be effective. The results of this study can help mine management make decisions relating to the development and the design of safe working places for both workers and machinery. Thus, it can be used to guide safe mining practices.

Funding information: This work was supported by the National Key R&D Program of China (Grant no: 2018-YFC0808202), and Major special project of Science and Technology in Shanxi Province (Grant no: 20181101013).

Author contributions: Conceptualization: H.D., S.H., and J.F.; methodology: H.D. and J.F.; formal analysis: D.P. and J.F.; funding acquisition: S.H., and Y.W.; resources: S.H. and J.F.; project administration: H.D.; supervision: D.P.; writing – original draft: H.D.; writing – review and editing: J.F. All authors have read and agreed to the published version of the manuscript.

Conflict of interest: The authors declare no conflict of interest.

Data availability statements: Some or all data, models, or code that support the findings of this study are available from the corresponding author upon reasonable request (list items).

References

[1] Wu Q, Zhou WF, Wang JH, Xie SH. Prediction of groundwater inrush into coal mines from aquifers underlying the coal seams in China: application of vulnerability index method to Zhangcun coal mine, China. Environ Geol. 2009;57:1187–95.
[2] Zhai LJ. Comprehensive exploration technology of water disaster prevention and control in coal mining roof. Procedia Earth Planet Sci. 2011;3:303–10.
[3] Zambrano LI, Sierra M, Lara B, Rodríguez-Núnez I, Medina MT, Lozada-Riascos CO, et al. Estimating and mapping the incidence of dengue and chikungunya in Hondurasduring 2015 using geographic information systems (GIS). J Infect Public Health. 2017;10:446–56.
[4] Jafar R, Shahrour I, Juran I. Application of artificial neural networks (ANN) to model the failure of urban water mains. Math Computer Model. 2010;57:1170–80.
[5] Chen W, Xie XS, Peng JB, Wang JL, Duan Z, Hong HY. GIS-based landslide susceptibility modelling: a comparative assessment of kernel logistic regression, Naïve-Bayes tree, and alternating decision tree models. Geomat Nat Hazards Risk. 2017;8:1–24.
[6] Korres WW, Schneider KK. GIS for hydrology. Cologne: Elsevier; 2017.
[7] Holguína LR, Sternberg T. A GIS based approach to Holocene hydrology and social connectivity in the Gobi Desert, Mongolia. Archaeol Res Asia. 2016;15:137–45.
[8] Wu Q, Xu H, Pang W. GIS and ANN coupling model: an innovative approach to evaluate vulnerability of karst water inrush in coalmines of north China. Environ Geol. 2008;54:937–43.
[9] Surinaidu L, Gurunadha, Rao VVS, Ramesh G. Assessment of groundwater inflows into Kuteshwar Limestone Mines through flow modeling study,Madhya Pradesh, India. Arab J Geosci. 2013;6:1153–61.
[10] Wu Q, Liu YZ, Liu DH, Zhou WF. Prediction of floor water inrush: the application of GIS-based AHP vulnerable index method to donghuantuo coal mine, China. Rock Mech Rock Eng. 2011;44:591–600.
[11] Wang SJ, Hou EK, Feng J, Wei YF, Zhao P. Partitioning prediction on the risk of water inflow(inrush) of no. 2 coal seam roof in Huangling no. 1 mine. J Xi'an Univ Sci Technol. 2012;32:155–9.
[12] Wu JS, Xu SD, Zhou R, Qin YP. Scenario analysis of mine water inrush hazard using Bayesian networks. Saf Sci. 2016;89:231–9.
[13] Wei JC, Li ZJ, Shi LQ, Guan YZ, Yin HY. Comprehensive evaluation of water-inrush risk from coal floors. Min Sci Technol (China). 2010;20:121–5.
[14] Liu ZB, Jin DW, Liu QS. Prediction of water inrush through coal floors based on data mining classification technique. Procedia Earth Planet Sci. 2011;3:166–74.
[15] Meng ZP, Li GQ, Xie XT. A geological assessment method of floor water inrush risk and its application. Eng Geol. 2012;143–144:51–60.
[16] Wang LG, Miao XX, Dong X, Wu Y. Application of quantification theory in risk assessment of mine flooding. J China Univ Min Technol. 2008;18:38–41.
[17] Duan HF, Jiang ZQ, Zhu SY, Zhao LJ, Liu JG. A expansive limits anti-permeability strength methodology of the coal mine floor water inrush evaluating. Procedia Environ Sci. 2012;12:372–8.
[18] Bukowski PWater. Hazard assessment in active shafts in upper Silesian coal basin mines. Mine Water Env. 2011;30:302–11.
[19] Li LP, Lei T, Li SC, Zhang QQ, Xu ZH, Shi SS, et al. Risk assessment of water inrush in karst tunnels and software development. Arab J Geosci. 2015;8:1843–54.
[20] Wang JS, Diao MZ, Yue KH. Optimization on pinch point temperature difference of ORC system based on AHP-Entropy method. Energy. 2017;141:97–107.
[21] Ma D, Bai HB. Groundwater inflow prediction model of karst collapse pillar: a case study for mining-induced groundwater inrush risk. Nat Hazards. 2015;76:1319–34.
[22] Pang YH, Wang GF, Ding ZW. Mechanical model of water inrush from coal seam floor based on triaxial seepage experiments. Int J Coal Sci Technol. 2014;4:428–33.
[23] Lu YL, Wang LG. Numerical simulation of mining-induced fracture evolution and water flow in coal seam floor above a confined aquifer. Comput Geotech. 2015;67:157–71.
[24] Huang L, Liu CY. Products of combustion of the Yan'an formation coal seam and their characteristics in the northeastern ordos basin. Acta Geologica Sin. 2014;88(9):1753–61.
[25] Hou EK, Tong RJ, Feng J, Che XY. Water enrichment characteristics of burnt rock and prediction on water loss caused by coal mining. J China Coal Soc. 2017;42(1):175–82.
[26] Dai GL, Zhou Y, Yang T, Liu ML, Gao Z, Niu C. Study on multifactor complex analysis method applied to watery of sandstone in Zhiluo formation. Coal Sci Technol. 2016;44(7):186–90.